Nanoparticle-based local translation reveals mRNA as a translation-coupled scaffold with anchoring function

Shunnichi Kashida, Dan Ohtan Wang, Hirohide Saito, Zoher Gueroui

Nanoparticle-based local translation reveals mRNA as translation-coupled scaffold with anchoring function

Shunnichi KASHIDA[1], Dan Ohtan WANG[2,3], Hirohide SAITO[4], and Zoher GUEROUI[1*]

[1] PASTEUR, Département de chimie, École normale supérieure, PSL University, Sorbonne Université, CNRS, 75005 Paris, France

[2] Institute for Integrated Cell-Material Sciences (iCeMS), Kyoto University, Yoshida-Honmachi, Sakyo-ku, Kyoto, 606-8501, Japan

[3] The Keihanshin Consortium for Fostering the Next Generation of Global Leaders in Research (K-CONNEX), Yoshida-Honmachi, Sakyo-ku, Kyoto-shi, Kyoto, 606-8501, Japan

[4] Department of Life Science Frontiers, Center for iPS Cell Research and Application, Kyoto University, 53 Kawahara-cho, Shogoin, Sakyo-ku, Kyoto, 606-8507, Japan

*Correspondence: zoher.gueroui@ens.fr

Abstract

The spatial regulation of mRNA translation is central to cellular functions and relies on numerous complex processes. Biomimetic approaches could bypass these endogenous complex processes, improve our comprehension of the regulation, and allow for controlling local translation regulations and functions. However, the causality between local translation and nascent protein function remains elusive. Here, we developed a novel nanoparticle-based strategy to magnetically control mRNA spatial patterns in mammalian cell extracts and investigate how local translation impacts nascent protein localization and function. By monitoring the translation of the magnetically localized mRNAs, we show that mRNA-nanoparticle complexes operate as a source for the continuous production of proteins from defined positions. By applying this approach to actin-binding proteins, we triggered the local formation of actin cytoskeletons and identified the minimal requirements for spatial control of the actin filament network. In addition, our bottom-up approach identified a novel role for mRNA as a translation-coupled scaffold for the function of nascent N-terminal protein domains. Our approach will serve as a novel platform for regulating mRNA localization and investigating the function of nascent protein domains during translation.

Significance Statement

The spatial regulation of mRNA translation is central to cellular functions. Yet no current approach has achieved the spatial control of mRNAs to reveal the direct causality between local translation and cellular processes. Here we develop a novel biomimetic control system that bypasses endogenous complex processes to analyse this relationship. We demonstrate the magnetic manipulation of mRNA conjugated to nanoparticles to spatially control translation-based protein synthesis. We examined how physical constraints can shape mRNA translation and identify a novel mechanism of spatial control. We found the general principles underlying the spatial regulation of actin cytoskeleton patterns by local translation. From a biological perspective, this phenomenon may represent a general mechanism of spatial control that cells use to produce functional diversity.

\body

Introduction

One essential element often missing to explain cell-fate control concerns the spatiotemporal regulation of gene expressions. Though DNA stay compacted in the nucleus, mRNA species are exported from the nucleus to precise locations in the cytosol before being translated. Translational control under mRNA spatial regulation significantly contributes to many important cellular processes, such as the establishment of polarity, asymmetric division, synaptic plasticity, and memory consolidation[1]. For instance, the local translation of actin-associated proteins from subcellular-localized mRNAs has been increasingly recognized as an important process for regulating the dynamic formation of the actin cytoskeleton during cell polarization[2–7]. Although biochemistry, genetics, cell imaging, biophysics, and "omics" approaches have increased our understanding of the molecules and reaction mechanisms involved in the mRNA localization and local translation, none of these approaches can distinguish the functional contribution of the spatiotemporal dynamics of the mRNA from the molecular signalling. Thus, the causality between local translation and cell function remains elusive. Being able to design a bottom-up approach to bypass subcellular transport systems and uncouple endogenous biochemical regulation from physical constraints could reveal the principles underlying complex biological systems. *In vitro* synthetic biology and cell-free systems are powerful approaches for understanding the physical constraints that shape gene expression networks such as molecular crowding, compartmentalization, and space (diffusion, gradient)[8–12].

However, understanding the spatiotemporal nature of translation is still challenging and requires the development of novel orthogonal methods for harnessing

biomolecule functions. Optogenetics, magnetogenetics, and nanoparticle-based technologies could provide spatiotemporal control of biomolecule activities, but these approaches remain mainly limited to the control of signalling pathways and transcription-based gene expressions[13–32] and have not yet achieved spatiotemporal translation control.

Here, we examined how magnetic control can be implemented to spatially manipulate mRNA localization and its translation. As a first step towards this goal, we developed an *in vitro* local translation model based on synthetic-mRNA conjugated magnetic nanoparticles (mRNA-NPs) to control translation-based protein synthesis in space within confined HeLa cell extracts (**Figure 1**). The mRNA-NPs were designed as movable mRNA-based protein factories upon magnetic control. When supplied with sufficient translational ingredients, they could continuously synthesize specific proteins with spatiotemporal control (**Figure 1**). We achieved spatial patterns of mRNA-NPs in confined HeLa cell extracts using magnetic forces to trigger asymmetric mRNA-NP string-like patterns (**Figure 1**). Using this platform, we simultaneously monitored the localized translation and the dynamic behaviour of the protein products. The results revealed that translation-coupled anchoring of the N-terminal nascent protein domains during the translation and mRNA localization can produce a local concentration of the functional protein domains. Its functional relevance to cell function is demonstrated by the striking differences in actin filament patterns that were triggered by simply rearranging an actin-binding protein domain toward the N-terminal or the C-terminal of the protein translated on the mRNA-NPs.

Results

Translation of mRNA - nanoparticle conjugates in HeLa cell extracts

As a first step towards the spatial manipulation of mRNA molecules using magnetic forces, we designed mRNA-conjugated magnetic nanoparticles (mRNA-NPs) and assessed their translation efficiency by monitoring green fluorescent protein (GFP) synthesis in HeLa cell extracts. Messenger RNAs encoding GFP were transcribed *in vitro* and biotinylated at their 3' end. The mRNAs were grafted onto the surface of streptavidin-conjugated superparamagnetic NPs (size 200 nm, see Methods) by mixing in high salt buffer at a stoichiometry of about 800-1600 mRNAs per NP (SI Appendix, **Fig. S1a**).

We next monitored GFP protein synthesis from mRNA-NPs in HeLa cell extracts, a model cytoplasm with a full complement of translational factors. To mimic the geometrical confinement by the cell membranes, the extracts and mRNA-NPs were encapsulated in spherical droplets dispersed in mineral oil with diameters ranging between 10-130 μm (Methods, SI Appendix**, Fig. S1b**). To assess the translational efficiency of the mRNA-NPs, we monitored the fluorescence of GFP translated from GFP-encoding mRNA-NPs in encapsulated extracts and found mRNA grafted on NPs as function of time (SI Appendix**, Fig. S2**). Thus, mRNA-NPs do not affect mRNA translatability and can be used for studying translation and protein synthesis.

Next, we assessed whether we could observe asymmetrically localized mRNA-NPs and their translation efficiency in the droplets. For the fluorescent detection of mRNA-NPs, Cy5-labeled biotin-mRNAs were supplemented with non-fluorescent biotin-mRNA during the conjugation with NPs (Methods). Droplets of cell extracts were transferred into a slide chamber at the vicinity of a permanent NdFeB magnet that generates a field of about 0.15 T and a gradient of 50 $T \bullet m^{-1}$ (Methods, **Figure 2a**).

Within a few seconds after applying the magnetic field, the dispersed mRNA-NPs became organized into micrometric string-like assemblies that were aligned perpendicularly to the magnet side of the droplet interface (**Figure 2b**). The droplets were incubated for 4 hours with or without the field, and their fluorescence intensity showed that translated GFP were homogeneously distributed within the droplets (**Figure 2c and** SI Appendix**, S2b**). This finding suggests that the newly synthesized GFP proteins were successfully released from mRNA-NPs and rapidly diffused throughout the encapsulated cell extracts. Relative GFP concentration showed that the efficiency of GFP synthesis was independent of the magnetic field, indicating that neither the magnetic field nor the string-like mRNA-NP assemblies perturbed the translation process (**Figure 2c and** SI Appendix**, S2b**). In order to have information about the spatial localization of ribosomes, we labeled the 28s rRNA subunits of the ribosomes by using ECHO-liveFISH probes[33]. In the absence of magnetic localization of the mRNA-NPs, we observed a strong background noise and a few natural hotspots (SI Appendix**, Fig. S3**). In contrast, we observed bright fluorescent signals co-localizing with mRNA-NPs in the presence of magnetic accumulation of the mRNA-NPs, which support an enrichment of the ribosomes on the mRNA-NPs, thus translation localization (SI Appendix**, Fig. S3**).

Monitoring of nascent proteins on localized mRNA-NPs

To better characterize the mRNA-NP complexes, we developed an assay to monitor protein synthesis on localized mRNA-NPs and designed a fusion protein permitting the use of nascent N-terminal GFP as a real-time reporter of local translation. We hypothesized that the translation duration of GFP-mCherry would be about twice that of GFP and will allow nascent GFP to monitor the location of its own mRNA until

the release of GFP-mCherry proteins (**Figure 2d scheme**). To investigate this hypothesis, the translation of mRNA(GFP-mCherry)-NPs was analysed using time-lapse microscopy. About 10 minutes after the reaction started, we first detected a GFP signal that was persistent for hours and matched the localized mRNA-NP pattern (**Figure 2e and 2f**). Furthermore, the GFP fluorescence within the droplets increased homogeneously, indicating that GFP-mCherry proteins were continuously translated and released from the mRNA-NPs (**Figure 2d, 2f,** SI Appendix**, S4 and Supplementary Movie 1 & 2**). After 70-80 minutes, the GFP signals on the mRNA-NPs reached a maximum and then slowly decayed, possibly because of the limited translational efficiency of the confined cell extracts. Regarding mCherry, its fluorescence started to increase homogeneously within the droplets 50 minutes after the reaction was initiated, in agreement with the slower mCherry maturation time (40 min) compared to GFP[34–36] (8 min, **Figure 2f, red curve and Supplementary Movies 1 & 2**). In addition, we did not observe any co-localization between mCherry and mRNA-NPs, confirming that GFP-mCherry fusion proteins did not stall or accumulate on NP surfaces.

These observations identified several remarkable properties of the local translation mediated by mRNA-NPs. One is that the mRNA-NPs function to locally and continuously produce GFP-mCherry proteins that are released and dispersed in the solution. Therefore, as we hypothesized, the accumulation of GFP fluorescence on mRNA(GFP-mCherry)-NPs indicates that nascent N-terminal GFP was spatially retained on the mRNA via ribosomes during mCherry synthesis (**see Schematic Figure 2d**). Thus, we could consider the N-terminal GFP as a transient fluorescent indicator of local translation from mRNA-NPs. To further investigate the link between protein synthesis and the spatial retention of the nascent protein domain, we next monitored

local GFP synthesis as a function of the length of the downstream sequence after the GFP sequence. We designed two RNA constructs whose downstream sequences were shorter and longer than mRNA(GFP-mCherry), respectively: mRNA(GFP-122aa) and mRNA(GFP-375aa-mCherry) (**Figures 2g and 2h**). We found a small and short-lived GFP protein accumulation on RNA-NPs during mRNA(GFP-122aa) translation (**Figures 2g,** SI Appendix**, S4** and **Supplementary Movie 3)**, but strong GFP protein accumulation on the NPs during mRNA(GFP-375aa-mCherry)-NPs translation (**Figures 2h,** SI Appendix, **S4** and **Supplementary Movie 4**). These data underlie that the spatial retention time of GFP on mRNA-NPs is correlated with the peptide elongation length during translation, as showed by the time delay difference between the GFP signal on mRNA-NPs and the GFP diffusion fraction in the droplet (**Figures 2i** and, SI Appendix, **S5**). The translation speed in the droplets was estimated to be about 0.2-0.6 aa/s (SI Appendix**,** SI Appendix**, Fig S5b** and **S5c**), thus 5-10 times slower than that previously measured in mouse ES cells[37]. We have attributed this difference to two factors[38,39]: first our cell extract preparations were diluted, and second, our experiments were performed at 30 °C which is lower than physiological temperature. From a biological perspective, this phenomenon may represent a simple translation-based retaining mechanism of proteins at the site of translation for a time span defined by the mRNA translation duration.

Spatiotemporal control of F-actin meshwork by localized mRNA translation

Next, we asked whether the spatial retention of the N-terminal protein domain on localized mRNA-NPs could produce downstream functional diversity. We chose actin cytoskeleton pattern formation because of its relevance to important functions of a living cell, its versatile patterns, and its high dynamic nature[40,41]. Many efforts have

been made on deciphering the molecular players involved in targeting and locally regulating actin-related mRNAs, yet current models are tightly dependent on the cellular context through multiple processes and regulators. We focused on a functional domain that is widely shared by the actin-binding protein superfamily, namely, the actin-binding domain of utrophin (hereafter, ABD), which is shared with Dystrophin and α-Actinin[42–45]. This 30 kDa domain contains two actin-binding sites to bind and stabilize actin filaments, and its GFP fusion protein can be used as an actin filament promoting factor and label[46]. We replaced the mCherry protein of the GFP-mCherry fusion with ABD (**Figure 3**).

To investigate the significance of the N-terminal position of ABD in the mRNA sequence, two mRNA fusions were developed in which the order of ABD and GFP was swapped (ABD-GFP and GFP-ABD) (**Figure 3a, left**). The mechanism of spatial retention permitted us to anticipate two situations: The translation of mRNA(GFP-ABD)-NPs were designed to spatially retain N-terminal GFP on the mRNA-NPs area and will produce GFP-ABD that diffuse immediately after synthesis; the translation of mRNA(ABD-GFP)-NPs were designed to spatially retain N-terminal ABD on the mRNA-NP area and then release ABD-GFP that diffuse homogeneously in the droplets (**Figure 3a**).

First, we checked the translation of these two mRNAs and their capacity to trigger the formation of actin filaments (F-actin). The two mRNAs (without conjugation to NPs) were translated for 3 hours in cell extract droplets supplemented with monomeric actin and fluorescent phalloidin, a probe for observing F-actin (SI Appendix**, Fig. S6**). We found that both mRNA constructs generate an interconnected F-actin meshwork (SI Appendix, **Fig. S6**). Phalloidin staining perfectly matched the translated ABD-GFP and GFP-ABD localization, which indicated that the respective

ABDs have the capacity to both promote and bind F-actin in the cell extracts (SI Appendix, **Fig. S6**).

To assess actin filament formation from the localized mRNAs, we next conjugated each mRNA construct with NPs (with 800:1 ratio) and assembled the mRNA-NPs into string-like patterns in confined extracts. Interestingly, when examining the translation of asymmetrically distributed mRNA-NPs, we found that the pattern of the F-actin meshworks was highly dependent on the N-terminal or C-terminal position of the ABD sequence on the mRNAs (**Figures 3b and 3c**).

The translation of localized mRNA(GFP-ABD)-NPs led to the formation of a homogenous F-actin meshwork without any local enrichment of the filaments at the vicinity of the mRNA-NPs (**Figure 3b zoom**), as indicated by the phalloidin signal (**Figure 3b**, **Cy5-mRNA-NPs and Phalloidin**). In addition, we also observed the GFP signal accumulate at the position of Cy5-labeled mRNA-NPs and confirmed the spatial retention of N-terminal GFP during downstream ABD local translation as in the case of GFP-mCherry (**Cy5-mRNA-NP and GFP-ABD in Figures 3b and** SI Appendix, **Fig. S7**). In contrast, the local translation of mRNA(ABD-GFP)-NPs showed a phalloidin signal that densely accumulated around Cy5-labeled mRNA-NPs, which suggested that the F-actin were locally nucleating by the spatially retained N-terminal ABD on mRNA-NPs (**Cy5-mRNA-NP and Phalloidin in Figure 3c zoom**). Moreover, string-like assemblies of mRNA-NPs displayed a more compact and denser pattern, as if the formation of a F-actin meshwork had modified the mRNA(ABD-GFP)-NP spatial organization (**Cy5-mRNA-NP and Phalloidin in Figures 3b and 3c zoom**). Though some diffused ABD-GFP molecules randomly promoted F-actin formation in the rest of the droplet, the locally translated ABD-GFP mainly co-recruited around the mRNA-NPs with the accumulating F-actin cytoskeleton (**Cy5-mRNA-NP,**

Phalloidin, and GFP-ABD in Figure 3c and SI Appendix, **Fig. S7**). The formation of localized F-actin mediated by the spatially-retained N-terminal ABD was also confirmed using time-lapse microscopy (**Figure 3d and Supplementary Movie 5**). F-actin accumulation on mRNA-NPs formed prior to non-localized actin formation, as revealed by the local enrichment in phalloidin staining at the early stage of translation (after about 10 minutes, **Figure 3d and Supplementary Movie 5**). The observation of an ABD-GFP-stained F-actin meshwork was detected later (after about 40 min), consistent with the timescale of the steady-state production of full-length ABD-GFP proteins (**Figure 3d**). Time-lapse observation also showed that the compacting of string-like assemblies of mRNA-NPs was correlated with the formation of localized F-actin meshworks (**Figure 3d and Supplementary Movie 5)**.

Altogether, these data showed that the N-terminal position of ABD in the mRNA sequence and mRNA localization in the droplet collaboratively dictated the micrometric local formation of the F-actin cytoskeleton.

Spatial retention of actin-binding proteins on hotspots of translational activity promotes reorganization of the actin filament meshwork

Our observations strongly suggest that mRNA(ABD-GFP)-NPs behave as hotspots of active ABD-covered NPs to promote local F-actin formation. In addition, we found that mRNA(ABD-GFP)-NP string-like patterns were changed upon local F-actin formation and eventually densely organized. Accordingly, we next examined how the spatial organization of mRNA-NP complexes can be regulated by their own protein products in the absence of external magnetic forces. We first examined how individual mRNA(GFP-ABD)-NPs and mRNA(ABD-GFP)-NPs could trigger different F-actin morphologies. As expected, the translation of mRNA(GFP-ABD)-NPs led to the

formation of a homogenous F-actin meshwork with a homogeneous spatial distribution of NPs within the droplets (**Figures 4a** and **4c**), as observed in **Figure 3b**. Time-dependent confocal observations distinguished the local translation activity on mRNA(GFP-ABD)-NPs, as indicated by the co-localization of Cy5-labeled mRNAs with GFP fluorescence (**Figures 4a, 4c,** SI Appendix, **Fig. S8, and Supplementary Movie 6 top**). In contrast, the translation of mRNA(ABD-GFP)-NPs led to a major spatial reorganization of mRNA-NPs as function of time (**Figures 4b, 4d, and** SI Appendix, **S8, and Supplementary Movie 6 bottom**). After 15 minutes, the initially homogeneous distribution of mRNA-NPs in the droplets started to form random micrometric clusters and eventually evolved into large assemblies within 45 minutes (**Figure 4d**). Interestingly, this spatial reorganization of mRNA-NPs was correlated with the spatial remodelling of the F-actin meshwork (**Figure 4d**). The formation of a hybrid meshwork composed of F-actin connected to NPs may explain the dynamic clustering of mRNA-NPs observed in Figure 4d and may account for the compaction of mRNA-NP string-like structures into dense organizations (**Figures 3c** and **3d)**. To test this hypothesis, we monitored the translation of non-biotinylated mRNA(ABD-GFP) in the presence of unconjugated NPs (SI Appendix**, Fig. S9 and Supplementary Movie 7**). In this case, F-actin formed a homogeneous meshwork coexisting with randomly distributed NPs, thus phenocopying the translation of mRNA(GFP-ABD)-NPs (SI Appendix**, Fig. S9 and Supplementary Movie 7**). These findings suggest that the multivalency provided by the multiple mRNA-NPs function as local hotspots for translational activity, which is required for the large-scale reorganization of F-actin meshworks in our system.

In conclusion, these data suggest that the spatial retention of ABD on hotspots for translational activity impact the spatiotemporal dynamics of F-actin assemblies, which

can, in turn, regulate the localization of mRNA-NPs. Thus, the temporary retention of ABD renders the mRNA complexes the ability to interact with their own coding proteins and downstream functional products.

Discussion

Our bottom-up approach is a first step towards the spatial control of mRNA translation using magnetic NPs, thus expanding the applications of magnetogenetics and NP-based technologies to RNA-based gene expression and spatial control. The designed mRNA-based complexes provide a novel platform for the spatial manipulation of local translation. This feature relies on two properties of the mRNA-NPs: first, by concentrating numerous mRNAs on an iron-oxide NP with defined stoichiometry, the mRNA-NPs behave as hotspots of local translation to continuously produce nascent proteins. Second, the mRNA-NPs can be manipulated by magnetic forces to generate localized spatial patterns. An exciting perspective of this work concerns the implementation of mRNA-NPs in cells and organisms where the spatiotemporal control of RNA translation is key to determining cell fate ~~behaviour~~.

Over the past years, several studies have identified how molecular players such as cis-acting RNA localization elements and RNA-binding proteins along with the transport of RNA granules by molecular motors along cytoskeletal fibers can act collectively to specifically regulate subcellular protein synthesis[1]. However, the mechanisms regulating the dynamic behavior and spatial positioning of the synthetized proteins upon translation termination and protein release remain elusive. To remain localized in a subcellular area, specific mechanisms are used by cells to counterbalance the diffusion and spreading in space of the newly synthetized proteins. For instance, protein anchoring to a localized scaffold at the site of translation and reduced mobility due to geometrical constraints or molecular crowding may confine proteins at the site of translation. Interestingly, in our study, by monitoring both local translation on mRNA-NPs and nascent fluorescent protein synthesis, we found that mRNA can act as an anchoring molecule that can spatially retain N-terminal folded protein domains

during translation. By examining the local translation of magnetic assemblies of mRNA-NPs coding for ABD, we found that the spatial retention of ABD at the mRNA-NP area was required to localize F-actin patterns (**Figures 3 and** SI Appendix**, Fig. S6**). These localized F-actin assemblies can, in turn, modify the localization of the mRNA-NP position, providing a feed-forward mechanism between localized mRNA translation activity and cytoskeleton self-organization (**Figure 4**). In this picture, the temporary spatial retention of ABD renders the mRNA-NP to interact with its own synthesized protein and functional partners (**Figure 5**). Experiments performed in bacteria and yeast have demonstrated that protein complexes can assemble while subunits are synthetized by the ribosome machinery co-translationally in cells[47–49]. In addition, recent studies have discovered novel functions of RNA as scaffolds that promote protein-protein interactions, with the 3' UTR of the mRNAs recruiting proteins to the site of translation to determine the subcellular protein localization[50], or with long non-coding RNA acting as platforms for post-translational functions[51]. Here, we show that the coding sequence of mRNA, in addition to providing genetic information, can also act as a scaffold molecule to localize protein-protein interactions between protein domains that fold during translation and binding protein partners (**Figure 5**).

The mechanism for spatially retaining protein domains during local translation may have relevant physiological implications. Given the modular organization of protein domain structures, a temporary local concentration of functional modules that are produced early in translation can be generated. Numerous actin-binding proteins have ABDs at their N terminals[42–45], suggesting the possibility of the spatial and temporal retention of the ABDs on mRNA templates for a duration defined by the extent of the downstream mRNA translation process. For instance, in humans, utrophin mRNAs and proteins are both known to be localized at neuromuscular junctions in

mouse muscle cells, and the long utrophin mRNA sequence downstream of the ABD (9537 bases which is 13 times longer than that of GFP) may thus serve as a scaffold to spatially retain ABD[42,43].

To conclude, our *in vitro* local translation model allowed us to identify possible anchoring functions of mRNA occurring co-translationally and mediated by the spatial retention of the N-terminal domain (**Figure 5**). Further investigations are needed to determine if this anchoring property occurs *in vivo* to enable localized protein-protein interactions by creating an enriched concentration of nascent functional protein domains that regulate local translation.

Materials and Methods

In vitro transcribed and biotin-end labelled mRNA were conjugated to streptavidin coated magnetic nanoparticles and encapsulated with HeLa cell extract in droplets. The droplets in a slide chamber besides NdFeB magnet were incubated at 30 °C and monitored under epifluorescence or confocal microscope. Phalloidin-568 was supplemented with the extract to visualize actin cytoskeleton formation. Detailed materials and methods are available in ***SI Appendix***.

Authors' contributions

S.K, D.O.W, H.S, and Z.G conceived and designed the experiments. S.K performed the experiments. S.K and Z.G analyzed the experiments. D.O.W and H.S contributed the materials/analysis tools. S.K and Z.G wrote the manuscript, and all authors commented on it.

Acknowledgements

We acknowledge the members of the Biophysical Chemistry group of ENS for fruitful discussions. We thank Dr. Kei Endo and Dr. Peter Karagiannis for reading carefully the manuscript. The authors also thank I. Oomoto, C. Parr, A. Hubstenberger, and Y. Fujita. S.K was supported by a fellowship, "bourse du gouvernement français". This work was supported by the HFSP Program Grant (RGP0050/2014) to D.O.W, H.S, and Z.G; by the CNRS to Z.G; and by the Ecole Normale Supérieure to Z.G.

Competing financial interests: The authors declare no competing financial interests.

References

1. Martin, K. C. & Ephrussi, A. mRNA localization: gene expression in the spatial dimension. *Cell* **136,** 719–730 (2009).
2. St. Johnston, D. Moving messages: The intracellular localization of mRNAs. *Nature Reviews Molecular Cell Biology* **6,** 363–375 (2005).
3. Condeelis, J. & Singer, R. H. How and why does β-actin mRNA target? *Biol. Cell* **97,** 97–110 (2005).
4. Hüttelmaier, S. *et al.* Spatial regulation of β-actin translation by Src-dependent phosphorylation of ZBP1. *Nature* **438,** 512–515 (2005).
5. Mingle, L. A. Localization of all seven messenger RNAs for the actin-polymerization nucleator Arp2/3 complex in the protrusions of fibroblasts. *J. Cell Sci.* **118,** 2425–2433 (2005).
6. Mili, S., Moissoglu, K. & Macara, I. G. Genome-wide screen reveals APC-associated RNAs enriched in cell protrusions. *Nature* **453,** 115–119 (2008).
7. Mardakheh, F. K. *et al.* Global Analysis of mRNA, Translation, and Protein Localization: Local Translation Is a Key Regulator of Cell Protrusions. *Dev. Cell* **35,** 344–357 (2015).
8. Tan, C., Saurabh, S., Bruchez, M. P., Schwartz, R. & Leduc, P. Molecular crowding shapes gene expression in synthetic cellular nanosystems. *Nat. Nanotechnol.* **8,** 602–608 (2013).
9. Hansen, M. M. K. *et al.* Macromolecular crowding creates heterogeneous environments of gene expression in picolitre droplets. *Nat. Nanotechnol.* **11,** 1–8 (2015).
10. Karzbrun, E., Tayar, A. M., Noireaux, V. & Bar-Ziv, R. H. Programmable on-chip DNA compartments as artificial cells. *Science (80-.).* **345,** 829–832 (2014).
11. Weitz, M. *et al.* Diversity in the dynamical behaviour of a compartmentalized programmable biochemical oscillator. *Nat. Chem.* **6,** 295–302 (2014).
12. Torre, P., Keating, C. D. & Mansy, S. S. Multiphase water-in-oil emulsion droplets for cell-free transcription-translation. *Langmuir* **30,** 5695–5699 (2014).
13. Toettcher, J. E., Voigt, C. A., Weiner, O. D. & Lim, W. A. The promise of optogenetics in cell biology: interrogating molecular circuits in space and time. *Nat Methods* **8,** 35–38 (2011).
14. del Pino, P. Tailoring the interplay between electromagnetic fields and nanomaterials toward applications in life sciences: a review. *J. Biomed. Opt.* **19,** 101507 (2014).
15. Del Pino, P. *et al.* Gene silencing mediated by magnetic lipospheres tagged with small interfering RNA. *Nano Lett.* **10,** 3914–3921 (2010).
16. Chen, R., Canales, A. & Anikeeva, P. Neural recording and modulation technologies. *Nature Reviews Materials* **2,** (2017).
17. Etoc, F. *et al.* Subcellular control of Rac-GTPase signalling by magnetogenetic manipulation inside living cells. *Nat Nano* **8,** 193–198 (2013).
18. Meister, M. *et al.* Physical limits to magnetogenetics. *Elife* **5,** 589–599 (2016).
19. Tay, A., Kunze, A., Murray, C. & Di Carlo, D. Induction of Calcium Influx in Cortical Neural Networks by Nanomagnetic Forces. *ACS Nano* **10,** 2331–2341 (2016).
20. Wheeler, M. A. *et al.* Genetically targeted magnetic control of the nervous system. *Nat. Neurosci.* **19,** 756–761 (2016).
21. Scherer, F. *et al.* Magnetofection: Enhancing and targeting gene delivery by magnetic force in vitro and in vivo. *Gene Ther.* (2002). doi:10.1038/sj.gt.3301624
22. Pankhurst, Q. A., Connolly, J., Jones, S. K. & Dobson, J. Applications of magnetic nanoparticles in biomedicine. *J. Phys. D-Applied Phys.* **36,** R167–R181 (2003).
23. Creixell, M., Bohórquez, A. C., Torres-Lugo, M. & Rinaldi, C. EGFR-targeted magnetic nanoparticle heaters kill cancer cells without a perceptible temperature rise. *ACS Nano* (2011). doi:10.1021/nn201822b
24. Cruz-Acuña, Melissa; Halman, Justin R; Kirill Afonin; Dobson, Jon ; Rinaldi, C. Magnetic nanoparticles loaded with functional RNA nanoparticles. *Nanoscale* **10,**

17761 (2018).
25. Mannix, R. J. & et al. Nanomagnetic actuation of receptor-mediated signal transduction. *Nat. Nanotechnol.* **3,** 36–40 (2008).
26. Cho, M. H. *et al.* A magnetic switch for the control of cell death signalling in in vitro and in vivo systems. *Nat. Mater.* **11,** 1038–43 (2012).
27. Huang, H., Delikanli, S., Zeng, H., Ferkey, D. M. & Pralle, A. Remote control of ion channels and neurons through magnetic-field heating of nanoparticles. *Nat Nanotechnol* **5,** 602–606 (2010).
28. Stanley, S. A. *et al.* Radio-Wave Heating of Iron Oxide Nanoparticles Can Regulate Plasma Glucose in Mice. *Science* **336,** 604–608 (2012).
29. Yamaguchi, M., Ito, A., Ono, A., Kawabe, Y. & Kamihira, M. Heat-Inducible Gene Expression System by Applying Alternating Magnetic Field to Magnetic Nanoparticles. *Acs Synth. Biol.* **3,** 273–279 (2014).
30. Hoffmann, C. *et al.* Spatiotemporal control of microtubule nucleation and assembly using magnetic nanoparticles. *Nat. Nanotechnol.* **8,** 199–205 (2013).
31. Chen, C. C. *et al.* DNA-gold nanorod conjugates for remote control of localized gene expression by near infrared irradiation. *J. Am. Chem. Soc.* **128,** 3709–3715 (2006).
32. Seo, D. *et al.* A mechanogenetic toolkit for interrogating cell signaling in space and time. *Cell* **165,** 1507–1518 (2016).
33. Oomoto, I. *et al.* ECHO-liveFISH: in vivo RNA labeling reveals dynamic regulation of nuclear RNA foci in living tissues. *Nucleic Acids Res.* **43,** 1–19 (2015).
34. Shin, J. & Noireaux, V. Study of messenger RNA inactivation and protein degradation in an Escherichia coli cell-free expression system. *J. Biol. Eng.* **4,** 9 (2010).
35. Svitkin, Y. V. *et al.* N1-methyl-pseudouridine in mRNA enhances translation through eIF2α-dependent and independent mechanisms by increasing ribosome density. *Nucleic Acids Res.* 1–14 (2017). doi:10.1093/nar/gkx135
36. MacDonald, P. J., Chen, Y. & Mueller, J. D. Chromophore maturation and fluorescence fluctuation spectroscopy of fluorescent proteins in a cell-free expression system. *Anal. Biochem.* **421,** 291–298 (2012).
37. Ingolia, N. T., Lareau, L. F. & Weissman, J. S. Ribosome profiling of mouse embryonic stem cells reveals the complexity and dynamics of mammalian proteomes. *Cell* **147,** 789–802 (2011).
38. Mikami, S., Kobayashi, T., Masutani, M., Yokoyama, S. & Imataka, H. A human cell-derived in vitro coupled transcription/translation system optimized for production of recombinant proteins. *Protein Expr. Purif.* **62,** 190–8 (2008).
39. Mikami, S., Masutani, M., Sonenberg, N., Yokoyama, S. & Imataka, H. An efficient mammalian cell-free translation system supplemented with translation factors. *Protein Expr. Purif.* **46,** 348–57 (2006).
40. Letort, G., Ennomani, H., Gressin, L., Théry, M. & Blanchoin, L. Dynamic reorganization of the actin cytoskeleton. *F1000Research* (2015). doi:10.12688/f1000research.6374.1
41. Pollard, T. D. & Cooper, J. A. Actin, a Central Player in Cell Shape and Movement. *Science (80-.).* **326,** 1208–1212 (2009).
42. Vater, R. *et al.* Utrophin mRNA expression in muscle is not restricted to the neuromuscular junction. *Mol. Cell. Neurosci.* **10,** 229–242 (1998).
43. Keep, N. H. *et al.* Crystal structure of the actin-binding region of utrophin reveals a head-to-tail dimer. *Structure* **7,** 1539–1546 (1999).
44. Borrego-Diaz, E. *et al.* Crystal structure of the actin-binding domain of α-actinin 1: Evaluating two competing actin-binding models. *J. Struct. Biol.* **155,** 230–238 (2006).
45. Roper, K. The `Spectraplakins': cytoskeletal giants with characteristics of both spectrin and plakin families. *J. Cell Sci.* **115,** 4215–4225 (2002).
46. Winder, S. J. *et al.* Utrophin actin binding domain: analysis of actin binding and cellular targeting. *J. Cell Sci.* **108 (Pt 1,** 63–71 (1995).
47. Shieh, Y. W. *et al.* Operon structure and cotranslational subunit association direct protein assembly in bacteria. *Science (80-.).* (2015). doi:10.1126/science.aac8171

48. Shiber, A. *et al.* Cotranslational assembly of protein complexes in eukaryotes revealed by ribosome profiling. *Nature* (2018). doi:10.1038/s41586-018-0462-y
49. Mayr, C. Protein complexes assemble as they are being made. *Nature* (2018). doi:10.1038/d41586-018-05905-4
50. Berkovits, B. D. & Mayr, C. Alternative 3′ UTRs act as scaffolds to regulate membrane protein localization. *Nature* **522,** 363–367 (2015).
51. Yoon, J. H. *et al.* Scaffold function of long non-coding RNA HOTAIR in protein ubiquitination. *Nat. Commun.* **4,** (2013).

Figure legends

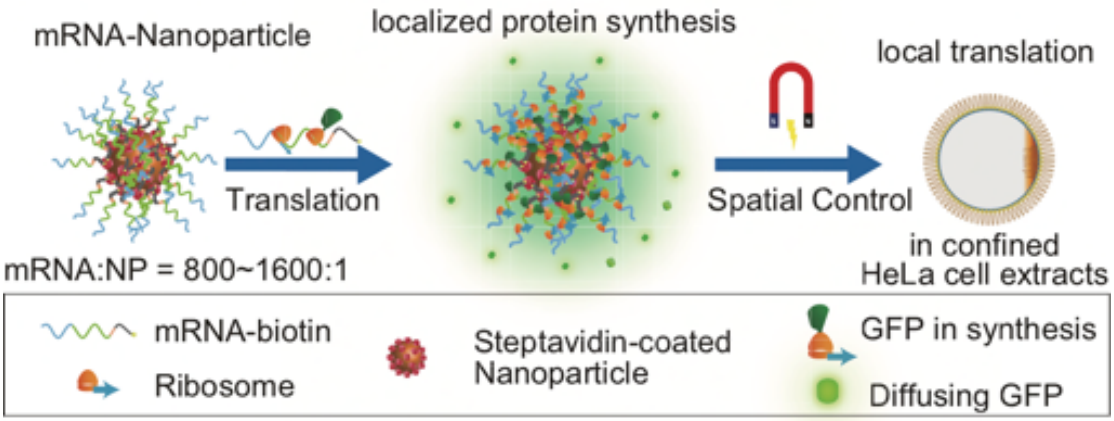

Figure 1. Magnetic nanoparticle-based spatiotemporal regulation of mRNA translation. Messenger RNAs conjugated to iron-oxide nanoparticles (mRNA-NPs) are designed as an RNA-based local source of protein synthesis, which combines the features of magnetic mobility and specific mRNA localization around the nanoparticle. The mRNA-NPs can continuously synthesize specific nascent proteins (e.g., GFP) and release them from the nanoparticles. The spatial control of mRNA-NPs is mediated by a magnetic field to generate mRNA localization in order to assess the effect of mRNA-NPs on local translation.

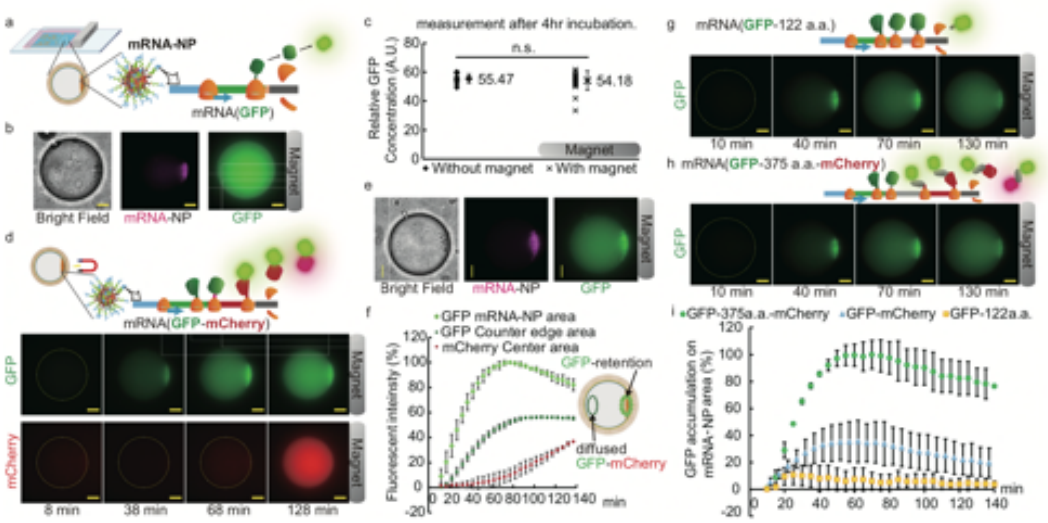

Figure 2. Translation of mRNA - nanoparticle conjugates in HeLa cell extract droplets. a-c GFP translation from localized mRNA-NPs. **a**, Schematic of the translation from asymmetrically localized mRNA-NPs performed in HeLa cell extract confined in droplets. The HeLa extract droplets were incubated in an observation chamber beside a permanent magnet. **b**, Epifluorescence microscopy observation of Cy5-labeled mRNAs conjugated to NPs and asymmetrically aligned perpendicularly to the magnet side of the droplet interface. The translation of mRNA-NPs produces GFP that homogeneously diffuse within the droplet. Scale bar, 20 µm (**b**). **c**, Relative GFP concentration measured in the droplets after 4 hours incubation with (n=52) or without (n=26) the magnet. **d-f** GFP-mCherry translation from asymmetrically localized mRNA-NPs. **d**, Top: Schematic of the translation process on localized mRNA-NPs. N-terminal nascent GFPs are anchored to mRNA-NPs via translating mCherry peptides and ribosomes. Bottom: Representative time-lapse images of translated GFP and mCherry with epifluorescence microscopy. **e**, Cy5-labeled mRNA on NPs colocalize with the translated GFP. **f**, Time-dependent evolution of the normalized mean fluorescence intensities of GFP and mCherry in selected regions of interest in the droplets (one frame every 5 minutes). Error bars represent standard deviation (SD). **g,h,**

Representative time-lapse images of translated GFPs from localized mRNA-NPs for mRNA(GFP-122a.a) and mRNA(GFP-375a.a.-mCherry), respectively. **i,** Time dependent evolution of the mean fluorescence intensity of accumulated GFPs on mRNA-NPs for mRNA(GFP-375a.a.-mCherry), mRNA(GFP-122a.a) and mRNA(GFP-mCherry).

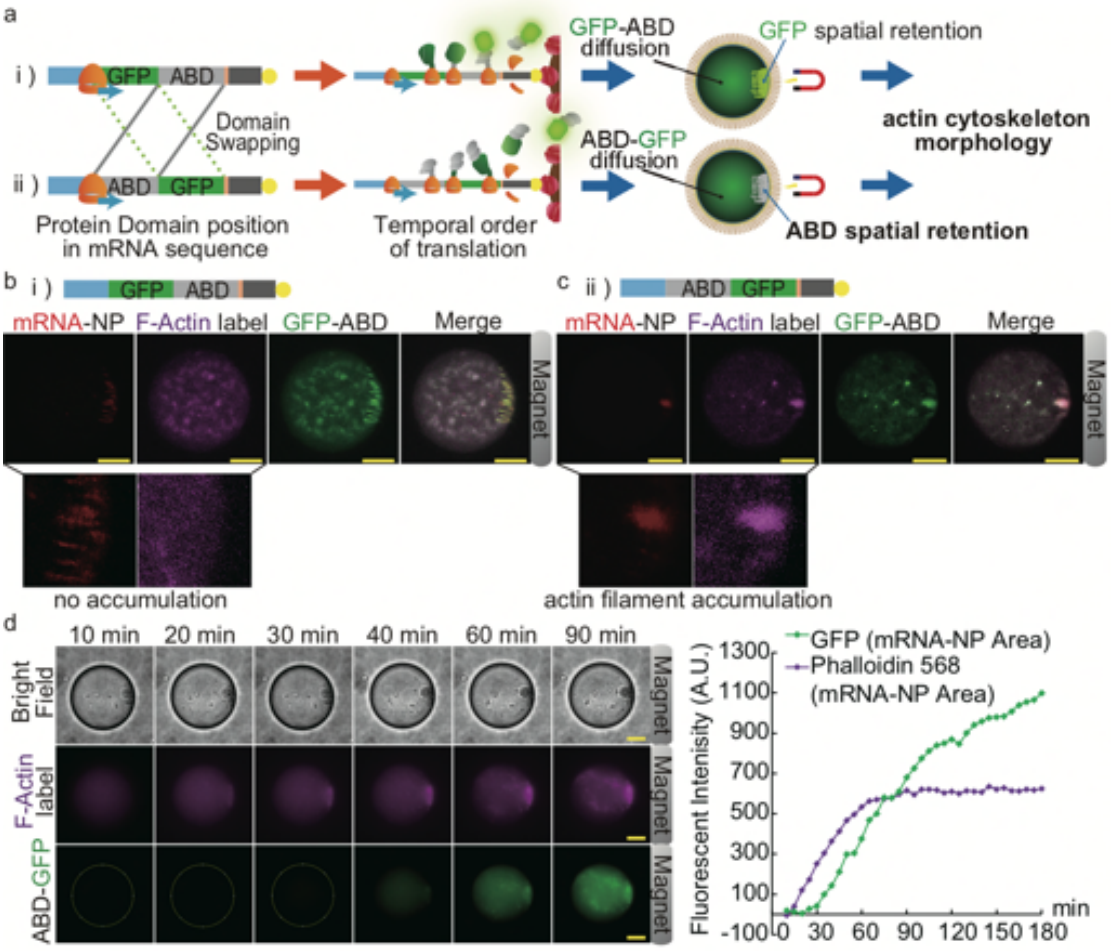

Figure 3. Spatial control of the F-actin meshwork by localized mRNA translation highlights key role of spatial retention of actin-binding protein. **a,** To assess the effect of the spatial retention of the N-terminal domain of actin-binding protein (ABD) during local translation on the actin filament assembly, two mRNA sequences were designed by swapping the order of ABD and GFP: ABD-GFP and GFP-ABD. These mRNAs were translated from localized mRNA-NPs in HeLa extract droplets. The translation of mRNA(GFP-ABD)-NPs was designed to spatially retain N-terminal GFP on the localized mRNA-NPs, whereas the translation of mRNA(ABD-GFP)-NPs was designed to spatially retain N-terminal ABD on the localized mRNA-NPs. **b, c,** Representative confocal fluorescence microscopy images of Cy5-mRNA-NPs,

Phalloidin-568 (F-actin marker), and GFP-ABD (**b**) or ABD-GFP (**c**) after 3 hours of translation. **b, zoom:** Formation of a homogenous F-actin meshwork without any local enrichment of filaments at the vicinity of the mRNA-NPs. **c, zoom:** Formation of a local and dense F-actin meshwork colocalizing with mRNA-NPs. **d.** Left panel: Representative time-lapse images of F-actin formation upon the translation of localized mRNA(ABD-GFP)-NPs. Right panel: Quantification of the mean fluorescence intensity of Phalloidin-568 and GFP signal as a function of time in the mRNA-NP area. Scale bars, 20 μm (**b-d**).

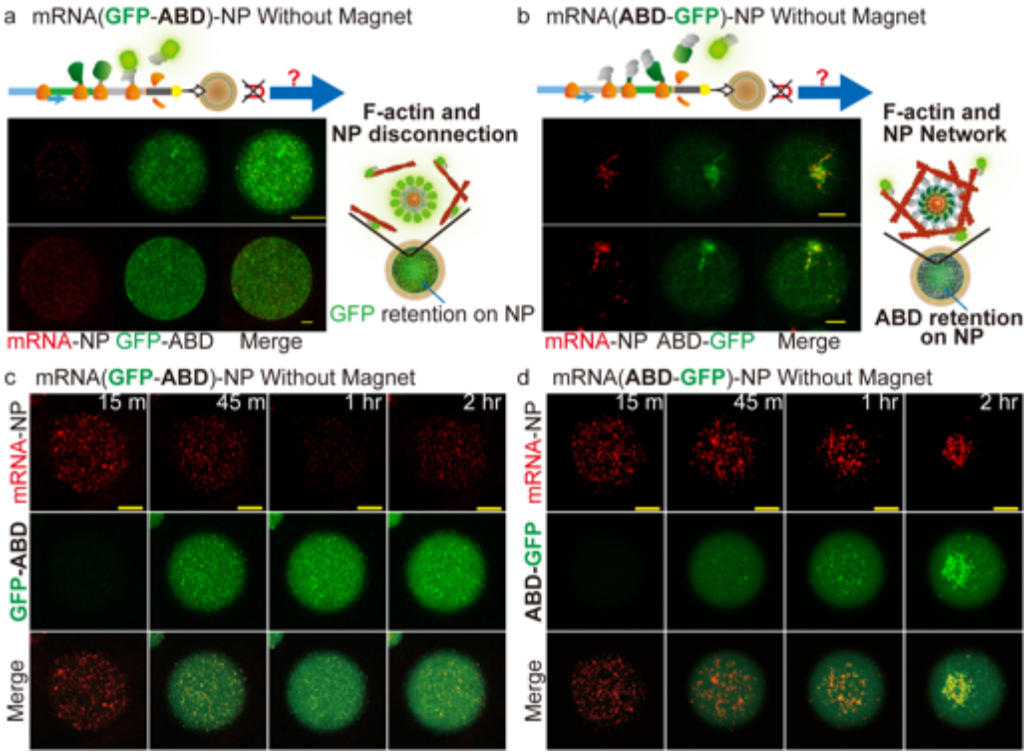

Figure 4. Spatial retention of actin-binding proteins on hotspots of translational activity promotes reorganization of the actin filament meshwork

a,b, Confocal observations of translation from mRNA(GFP-ABD)-NPs (**a**) and mRNA(ABD-GFP)-NPs (**b**) to assess how the spatial organization of mRNA-NP complexes can be regulated by their own protein products. Observations were performed after two hours of translation. The F-actin meshwork is labeled by GFP-ABD and mRNA-NPs by Cy5 labeled-mRNAs. **c,d,** Time-lapse observations of the dynamics of mRNA translation and mRNA-NP complexes **c,** N-terminal GFP signals (green) are localized on mRNA(GFP-ABD)-NPs (red, Cy5 labeled-mRNAs) after 45 minutes of translation. mRNA-NPs are spatially distributed in the droplet, and GFP-ABD-bound actin filaments form a homogenous meshwork. **d,** Translation of mRNA(ABD-GFP)-NPs leads to a spatial reorganization of mRNA-NPs as a function of time: mRNA(ABD-GFP)-NPs (red) and ABD-GFP (green) bound to actin filaments spontaneously accumulate together to form a dynamic meshwork that remodels spatially. Scale bars, 20 µm.

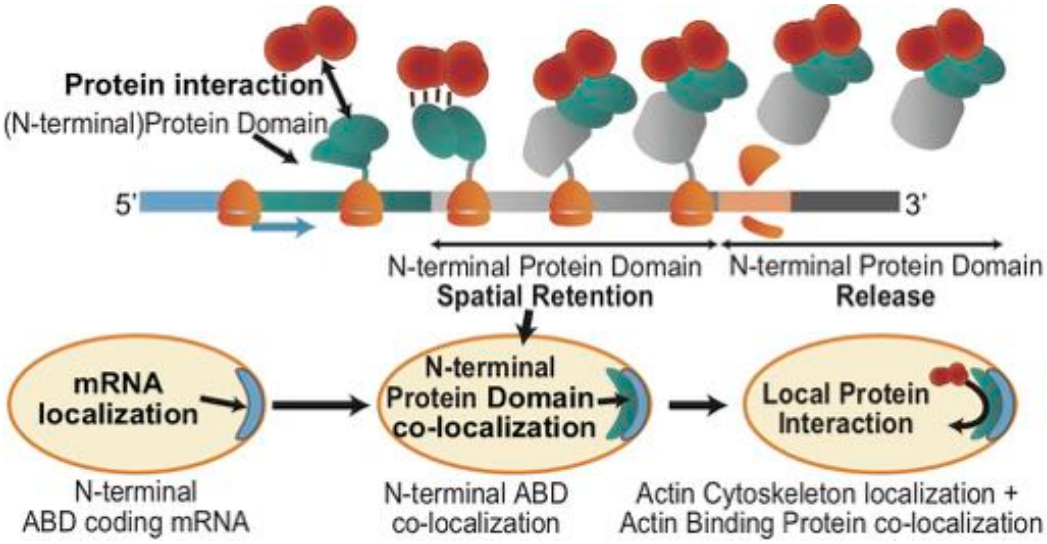

Figure 5: Proposed model of mRNA as translation-coupled scaffold with anchoring function to spatially constrain protein interactions

Spatially contrained protein interactions could be co-translationally mediated by the spatial retention of nascent protein domains on localized mRNA. For instance, the N-terminal position of the actin binding domain sequence on localized mRNA leads to the spatial retention of the protein domain during translation and eventually promotes actin filament localization.